Supplementary Information (SI) for Journal of Materials Chemistry C.

Supporting Information

Bidirectional luminescence modulation of BTO: Yb/Er ferroelectric films based on phase transition

Yu Qin,[ab] Yuping Jia,*[ab] Rui Sun,[ab] Entao Zhang,[ab] Hang Zang,[ab] Yulei Chang,[ab] Yitong Che,[ab] Mingrui Liu,[ab] Minchuan Liang,[ab] Xiaojuan Sun,*[ab] and Dabing Li, [ab]

[a] State Key Laboratory of Luminescence Science and Technology, Changchun Institute of Optics, Fine Mechanics and Physics, Chinese Academy of Sciences, Chang Chun, 130033, China.
[b] School of optoelectronics, University of Chinese Academy of Sciences, Beijing, 100049, China.

*Corresponding author email: ypjia@ciomp.ac.cn, sunxj@ciomp.ac.cn.

Rietveld refinement of the XRD pattern for the BTO: Yb/Er film was shown in Fig. S1, using a two-phase model (P4mm and R3m). The observed data (red dots), calculated profile (black line), and difference curve (blue line) are shown, along with the Bragg positions of the two phases (green and pink tick marks). The refinement results yield phase fractions of 50.09% for the tetragonal phase and 49.91% for the rhombohedral phase, with good fitting quality (R_p = 2.08%, R_{wp} = 2.65%, X^2 = 1.18), confirming the coexistence of T and R phases in the BTO: Yb/Er film.

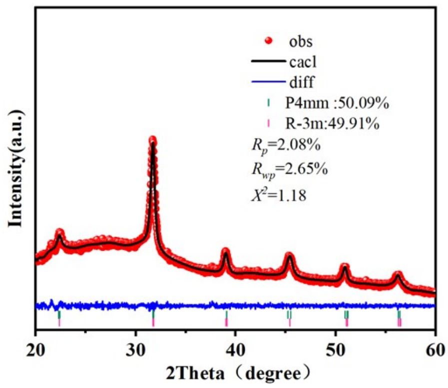

Figure S1. Rietveld refinement of the XRD pattern for the BTO: Yb/Er film.

We carried out Rietveld refinement of the XRD data. The calculated lattice parameters for the tetragonal phase are determined to be a = 3.9988 Å, b = 3.9988 Å, c = 4.0222 Å, compared to the bulk values of a = 3.994 Å, b = 3.994 Å, c = 4.038 Å.

Based on these values, the in-plane strain (ε_a) and out-of-plane strain (ε_c) can be calculated as:

$$\varepsilon_{\mathrm{a}} = \frac{a_{film} - a_{bulk}}{a_{bulk}} = \frac{3.9988 - 3.994}{3.994} \times 100\% \approx 0.12\%$$

$$\varepsilon_c = \frac{c_{film} - c_{bulk}}{c_{bulk}} = \frac{4.0222 - 4.038}{4.038} \times 100\% \approx - 0.39\%$$

These results confirm the presence of in-plane tensile strain and out-of-plane compressive strain.

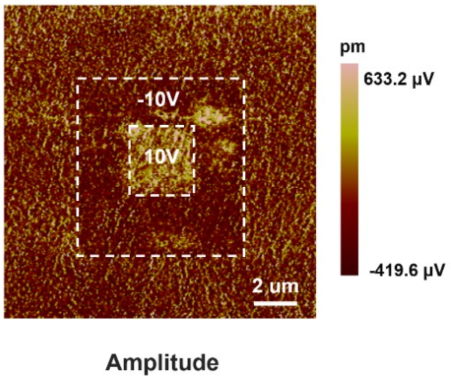

Figure S2. The out-of-plane PFM amplitude images of BTO: Yb/Er films at +10 V and -10 V are acquired over regions of 2×2 μm^2 and 5×5 μm^2

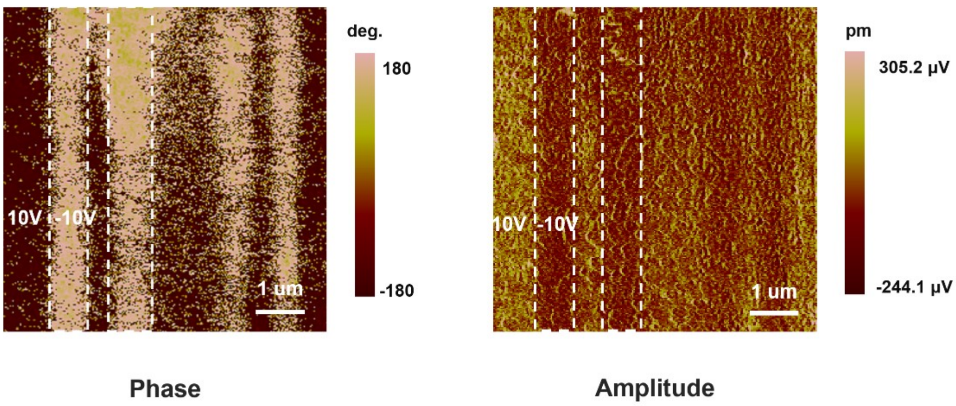

Figure S3. The phase and amplitude images of stripe area in 5×5 μm^2 region on BTO: Yb/Er films under applied voltages of +10 V and -10 V.

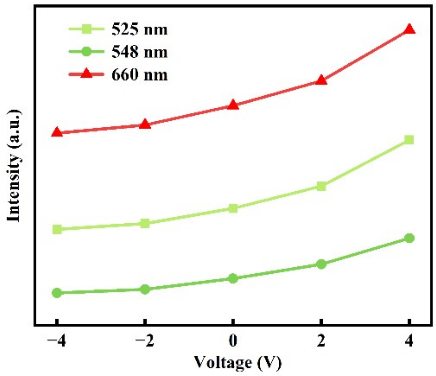

Figure S4. The bidirectional variation trends of different emission peaks in the photoluminescence (PL) spectra of BTO: Yb/Er films under 980 nm excitation as a function of applied voltage.

The fatigue tests were conducted using a ferroelectric tester (Radiant Precision Premier II). A square waveform with a peak voltage of 3V was applied at a frequency of 10Hz. The waveform width was set to 50ms positive and 50ms negative.

The total fatigue cycling was performed sequentially in cumulative segments, up to a maximum of 10^6 cycles. After each stress period, the remanent polarization (Pr) was extracted using the PUND (Positive-Up-Negative-Down) method with a volt of 9 V, a pulse width of 0.1ms, and a pulse delay of 1ms, as shown in Fig. S5. This setup allowed reliable separation of switchable polarization from non-ferroelectric contributions. The measured Pr values show negligible degradation after 10^6 cycles, indicating good fatigue endurance.

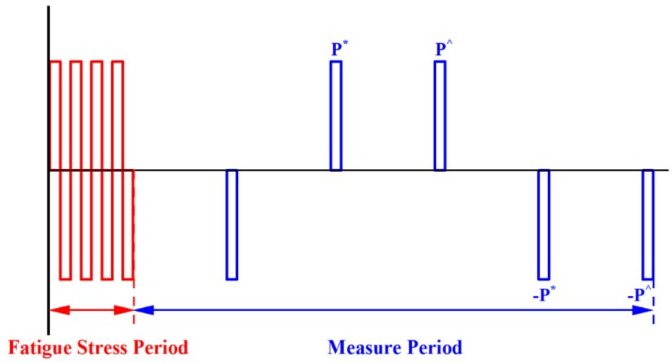

Figure S5. The fatigue signal profile, including a fatigue stress period and a PUND-based polarization measurement.

The P-E hysteresis loops measured before and after the fatigue test are presented in Fig. S6. As shown, the two curves exhibit only minimal differences. This observation is consistent with the fatigue result shown in Fig. 2e, where the remanent polarization (Pr) remains nearly unchanged after 10^6 switching cycles.

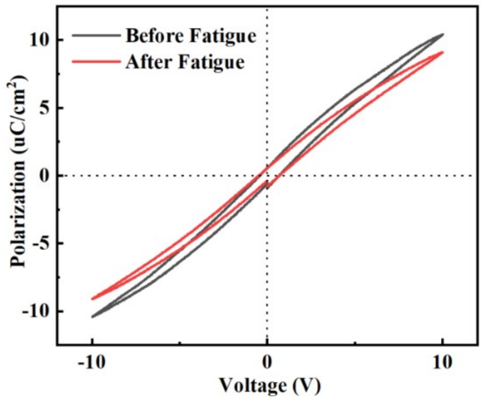

Figure S6. P–E hysteresis loops of the BTO: Yb/Er thin film measured before (black) and after (red) fatigue test.

Each diffraction curve shown in Fig. 4a, measured from BTO: Yb/Er thin films under different applied voltages (from –4 V to +4 V), was fitted using a multi-peak Gaussian function over the 2θ range of 44°–46°. The fitting clearly resolves three distinct peaks corresponding to the (002)T, (200)R, and (200)T respectively. The fitting parameters include peak positions (2θ), full width at half maximum (FWHM), intensities, and integrated areas for each peak under all voltage conditions. The goodness of fit is confirmed by high R2 values (>0.95) for all fitting cases, indicating a strong agreement between the experimental data and the fitted curves. All the parameters are now summarized in Table S1 and Table S2 for clarity and completeness.

Table S1. Fitting quality metrics under different applied voltages.

Voltage (V)	**Adjusted R^2**	**Data Points**	**Degrees of Freedom**
-4	0.95338	468	462
-2	0.95547	468	462
0	0.95409	468	462
2	0.95559	468	462
4	0.95158	468	462

Table S2. Gaussian fitting parameters of each diffraction peak at different voltages.

Voltage (V)	Peak	2θ (°)	FWHM (°)	Height	Area
-4	(002)T	44.6791	0.6147	247.63	162.03
	(200)R	45.2930	0.5325	591.53	335.29
	(200)T	45.6160	0.3506	246.27	91.91
-2	(002)T	44.7030	0.6062	241.16	155.62
	(200)R	45.2930	0.5125	569.27	310.57
	(200)T	45.5903	0.3448	266.48	97.80
0	(002)T	44.7372	0.6533	238.98	166.20
	(200)R	45.2930	0.5042	522.09	280.21
	(200)T	45.5680	0.3700	269.02	105.95
2	(002)T	44.7543	0.8073	282.73	242.97
	(200)R	45.2930	0.5210	452.13	250.75
	(200)T	45.5652	0.4385	315.60	147.32
4	(002)T	44.7933	0.9330	289.51	287.52
	(200)R	45.2930	0.5436	348.37	201.58
	(200)T	45.5303	0.4960	339.23	179.09